Int. J. Electrochem. Sci., 8 **(2013)** 390- 405

International Journal of
ELECTROCHEMICAL
SCIENCE
www.electrochemsci.org

Technical Report

Galvanic Behavior of Reinforced Concrete Before and After Repairs with Selective Use of 304 Stainless Steel

P. Castro-Borges[1,*], *M. Córdova*[2]

[1] Centro de Investigación y de Estudios Avanzados del IPN Unidad Mérida, Km 6 Antigua Carretera a Progreso, CP 97310, Cordemex, Mérida, Yucatán, México,
[2] Av. Industrias no Contaminantes por Periférico Norte, Apdo. Postal 15, Cordemex, Mérida, Yucatán, México
[*]E-mail: pcastro@mda.cinvestav.mx

Received: 5 October 2012 / *Accepted:* 30 November 2012 / *Published:* 1 January 2013

The galvanic couple effect decreases a few weeks after performing local repairs, nonetheless, there is few information on the effect the anodic/cathodic area (aA/aC) ratio has on the magnitude of the galvanic couple. The selective use of stainless steel represents an alternative to repair concrete structures, but it remains understudied, particularly in tropical marine environments of the Gulf of Mexico. In this paper, the influence of the anodic/cathodic area ratio on the galvanic behavior, before and after local repairs, conducted on small beams made of low-quality concrete and 304 stainless steel (SS) bars is analyzed and discussed. Some of the results from this experiment indicate that an aA/aC ratio of more than five causes a significant decrease in the galvanic couple of the adjacent areas.

Keywords: anodic/cathodic area, galvanic couple, repair, stainless steel.

1. INTRODUCTION

The use of stainless steel as a repair material in corrosion-damaged concrete structures remains as a controversial subject. In order to evaluate the use of stainless steel for such end, further research should look at: the effectiveness of the material used in the repair, the effects this material has on the repaired structure, and how the material's electrochemical behavior affects the existing carbon steel in the repaired structure. In this study, we evaluate the electrochemical effectiveness of using 304 SS to partially substitute the reinforcement on small corrosion-damaged concrete beams exposed to an aggressive marine environment simulated under laboratory conditions. Such evaluation was conducted shortly before and after repairs were performed (i.e., early-stage electrochemical behavior). The main objective was to determine the influence of the anodic/cathodic area ratio on the galvanic couple of

local repairs in concrete beams for which black steel had been replaced by 304 SS. Galvanic couple before repairing was also analyzed.

2. TESTING METHODOLOGY

We manufactured under laboratory conditions four reinforced concrete beams of 15 by 15 cm of section and 56.5 cm in length. Specimens were designed based on the most common type of section (rectangular or square) used in the Yucatan Peninsula, especially for school buildings. Reinforced concrete beams with a square section were made with four carbon steel bars, no stirrups, but electrically-connected by cables exposed at the end of the beam which joined the four reinforcement bars. These beams imitated existing structures located on the Gulf of Mexico coast, and were exposed to a simulated coastal marine environment under controlled laboratory conditions. On the other hand, specimens made with a square section were much easier to monitor in terms of corrosion parameters. The beams had three unsegmented bars and another segmented one. The latter was divided into three central sections of 10.5 cm each, and one external section of 11.5 cm on each side. All the reinforcement bars were made of carbon steel of 3/8 inch (0.95 cm) in diameter and degree 42. Unsegmented bars were numbered clockwise, starting with the bar that would be exposed to chlorides. On the other hand, the four segmented bars were named as 1s, 2s, 3s and 4s. Figure 1 shows a schematic representation of a beam with its segmented bar, as well as unsegmented bars.

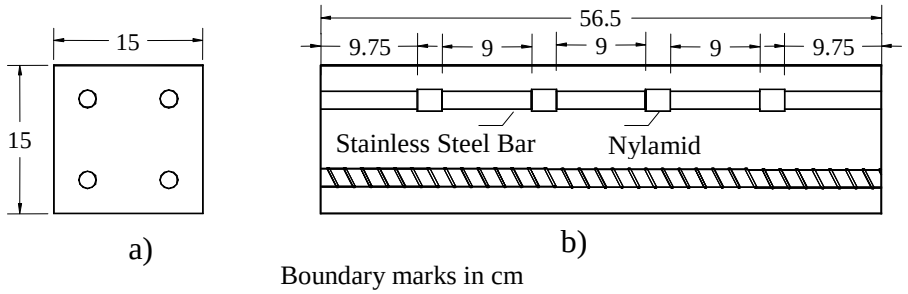

Figure 1. Example of a segmented bar in a beam; values are in cm. a) front view, b) lateral view.

Each segmented bar had five sections joined by a nylamid connector bar (nylon polymer) 1/2" (1.27 cm) in diameter and 1" (2.54 cm) in length, which was drilled inside in order to fit the steel bar (3/8" = 0.95 cm in diameter). The segments also had cables at the end in order to conduct measurements for each segment. Sections were numbered from 1 to 5 and named: SI, SII, SII, SIV and SV. Once all the segments had been fitted in the nylamid, epoxy resin was placed in the joints to provide stability and rigidity to the segmented bar. The concrete mix used was made with a local Portland cement (ASTM type I) and the mix design was based on the ACI design method by absolute volumes, considering a water/cement ratio of 0.60 and a total cement content of 307 kg/m^3. No additives or bonding materials were used for concrete adherence. The beams were cured for 7 days. The compressive strength resulted in a f'_c= 23,5 MPa. All four beams were exposed to accelerated

corrosion and then repaired following the traditional method. Figure 2 shows the final arrangement for beams with segmented and un-segmented bars.

Group I			
Beam #	**Bar #**	**Exposed bar**	
1	1,2,3,4	1	Continuous (SIII)
2	5,6,7,8	5	Continuous (SIII)
3	9,10,11,12	9	Continuous (SIII)
4	13,14,15,16	13	Continuous (SIII)
5	17,18,19,20	17	Continuous (SIII)
6	21,22,23,24	21	Continuous (SIII)

Group II		
Beam #	**Bars**	**Exposed bar**
7	1s,25,26,27	1s Segmented (SIII)
8	2s,28,29,30	2s Segmented (SIII)
9	3s,31,32,33	3s Segmented (SIII)
10	4s,34,35,36	4s Segmented (SIII)

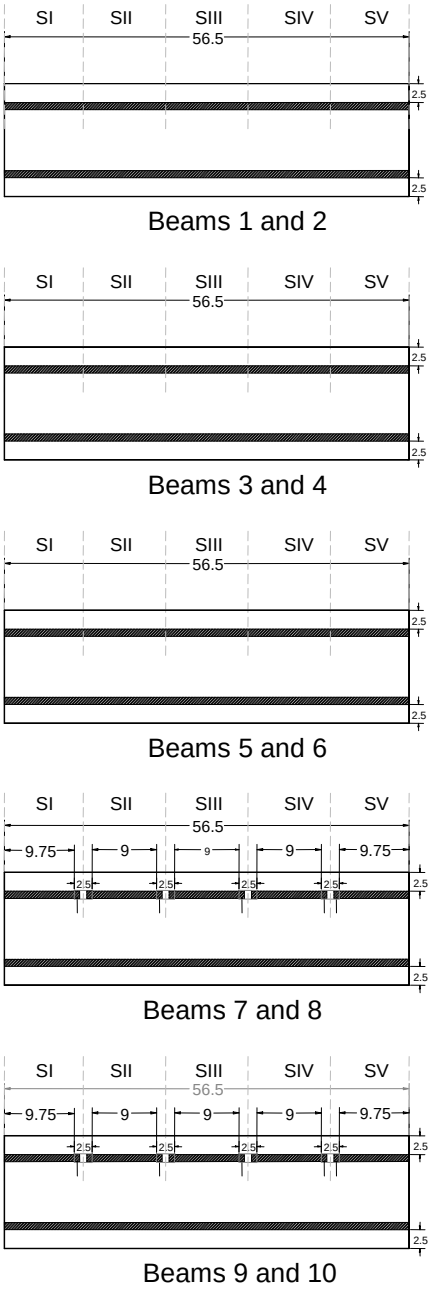

Figure 2. Final arrangement for beams with segmented and continuous bars.

2.1 Experimental procedure to measure galvanic currents

Galvanic current (Ig) was measured for all four beams by means of a zero resistance ammeter (ZRA), which is capable of giving the anodic and/or cathodic contribution of each measured bar [1]. Measurements were conducted by introducing the ZRA between the segments. According to Figure 3,

to obtain the first datum, cable 1 was connected to segment 1, and cable 2 was connected to the other inter-connected segments. This allowed us to measure the galvanic current value between segments 1 and 2. See Figure 3 for details. In order to obtain the Ig between segments 2 and 3, segments 1 and 2 were connected to cable 1, and segments 3, 4 and 5 were connected to cable 2. This allowed us to measure the galvanic current of all 5 segments. The segmented bar was disconnected from the other three unsegmented ones during galvanic current measurements for each segment.

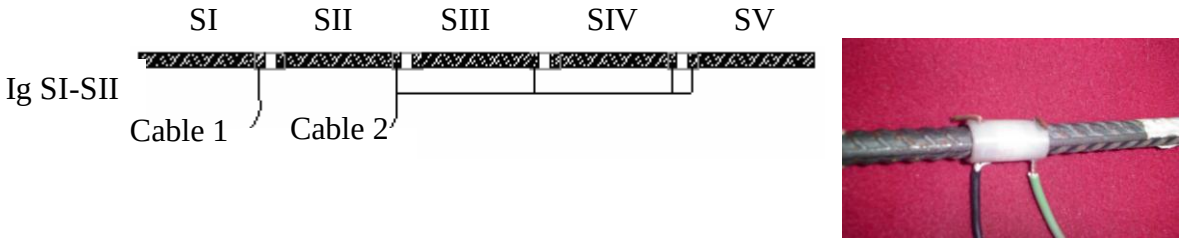

Figure 3. Closer look of a segmented bar and one of the connection arrangements.

The resulting values from the ZRA measurements were the galvanic current contributions of each segment or bar, and this is why the first value shown by the ZRA was taken as that of the first segment. To calculate the Ig, we calculated the arithmetical difference between the galvanic currents for segments 1 and 2, which in this case was taken to be the Ig for segment 2. This method was used to calculate the Ig values for all the other segments [1- 3].

2.2 Anodic/Cathodic area ratio (aA/aC)

The period prior to repairing was named BR (before repairing) while that after repairs had been conducted was named AR (after repairing), and included the first days of curing. Results were described in four stages based on relevant conditions and changes occurring at different moments after the repair had been conducted. Stage 1: period of time before the repair had been performed (BR). This stage lasted from the beginning of the wetting and drying cycles to the first moment at which a greater difference in galvanic current (between anode and one of the cathodes) between the affected bar and any of the others was detected. During this period, the concrete had a high level of humidity due to the wetting and drying cycles, and thus presented high galvanic current values. Stage 2: period of time which took place before the repair had been conducted (BR), and lasted from the moment at which the greater difference in galvanic current was first found to the end of the wetting and drying cycles. This stage was very important since it also showed a decrease in the galvanic couple due to an activation of the bars which are assumed to be cathodes due to chloride contamination that has started to reach them, resulting in high potential and corrosion rate values. Stage 3: period of time that included the repair and curing of the repair (AR). It is during this period that greater galvanic current values start to appear. Concrete humidity is high due to curing conditions. Stage 4: this period of time corresponded

to the last measurement taken on the repaired beams; at this time the Ig started stabilizing towards smaller values than those observed shortly after the repair had been made. During this stage, concrete humidity has decreased because the curing has already previously finished, and subsequent exposure cycles have not yet begun.

In the present investigation, we were able to observe that there is an initial condition that occurs during stages 1 and 2, when chlorides penetrate the concrete, in which anodic and cathodic areas are formed and have a certain magnitude of effect that takes place while the aggressive conditions last or until a repair is performed. After a repair has been conducted, anodic (active carbon steel) and cathodic (stainless steel 304) areas are defined, and this is why it is possible to study the influence this relationship has on the electrochemical behavior of repaired structures during stages 3 and 4.

The aA/aC relations used here were obtained according to electrochemical measurements taken from the exposed bars. Therefore, in agreement with the convention of signs previously fixed, when taking the measurements with the galvanostate, anodic (positive) and cathodic (negative) values were recorded and were assigned to each segment within each bar. Thus, the galvanic behavior of each segment was characterized for all of the repaired bars.

Once the anodic and cathodic values had been recorded for each section of the segmented bar, anode-cathode relations were calculated.

2.3 Specimens exposure to wet and dry cycles with sodium chloride

Once specimens were in a passive state, pre-corrosion was promoted in one corner of each beam through wet and dry cycles. The corners exposed to the wet and dry cycles were those corresponding to bars 1, 5, 9, 13, 17 and 21 from the group 1, and 1s, 2s, 3s and 4s from the group 2. The complete cycles had duration of 24 h:

Wetting: each of the 10 beams was positioned on a wood base whose purpose was to expose the selected corner of the beam (that to be repaired later) (see Figure 4). The central part of the corner was exposed to a 3.5% $NaCl^-$ solution by means of a wet sponge.

a)

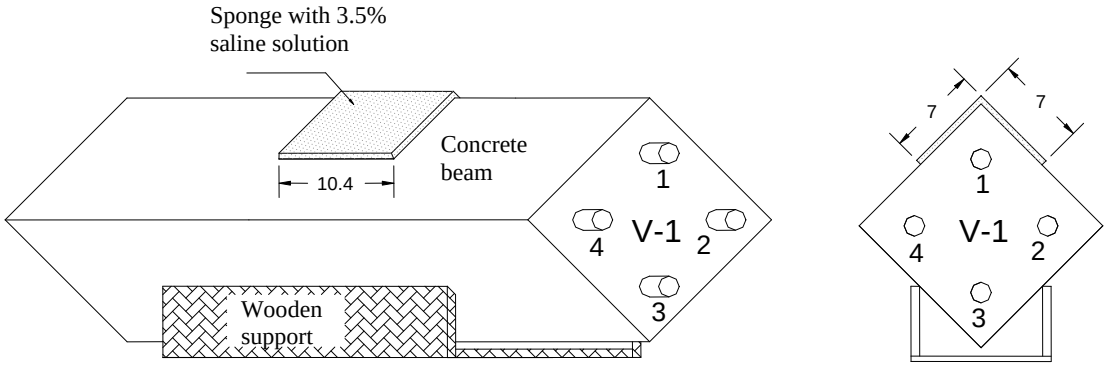

b)

Figure 4. Sketch (a) and photo (b) of beams during wet and dry cycles

One single corner of each beam was exposed to the aggressive condition to simulate what usually occurs under real conditions in the Port of Progreso, Yucatán, where breeze blows from the NE [4]. Galvanic current was measured after finishing the wetting stage.

Drying: the drying stage started once measurements were performed. Beams were positioned in a dry oven at constant temperature (50 C) during 24 h.

The same procedure was performed during 48 days until reaching the desired corrosion potential and rate

3. RESULTS

Figures 5 to 10 show the Ig behavior of beams from Group 1. Measurements do not show significant differences between anodic and cathodic values at the beginning of the exposure. However, after the third cycle, bars 1, 5, 9, 13, 17 and 21 started to show a strong anodic character which decreased little by little.

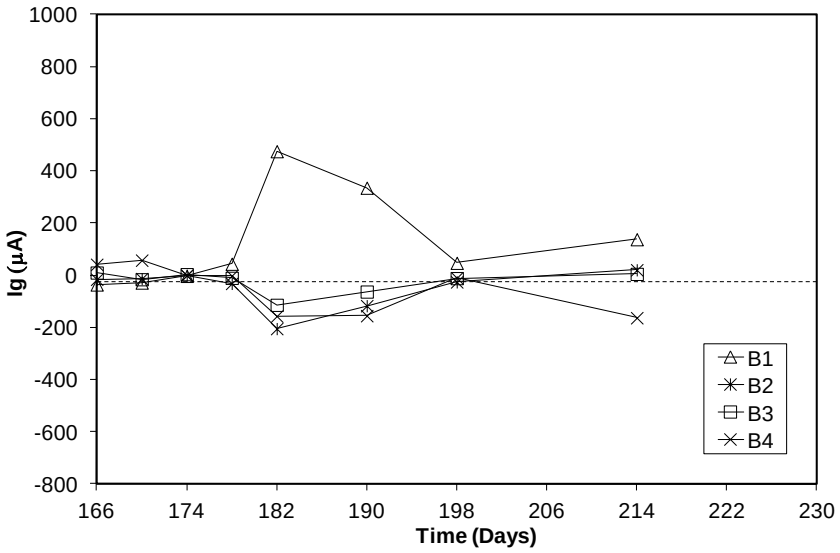

Figure 5. Plot of Ig for bars from Beam 1 (group 1). Positive zone is anodic and negative zone is cathodic.

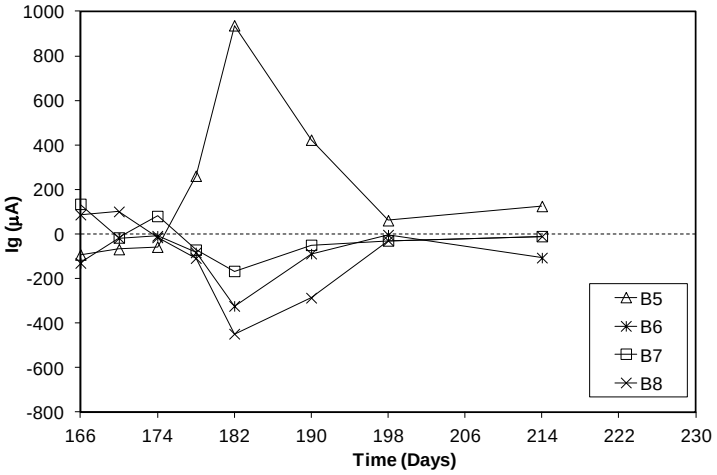

Figure 6. Plot of Ig for bars from Beam 2 (group 1). Positive zone is anodic and negative zone is cathodic.

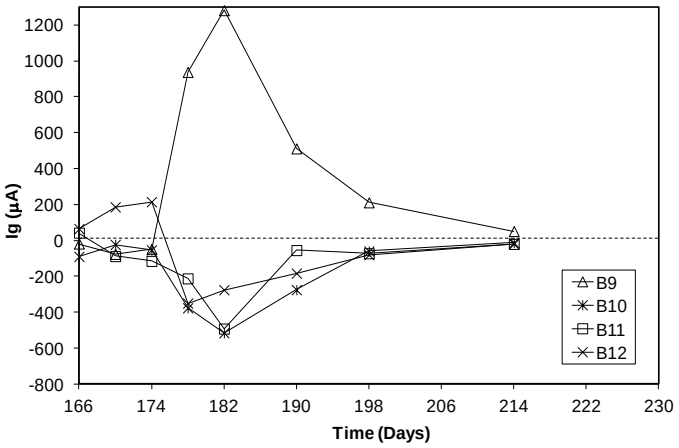

Figure 7. Plot of Ig for bars from Beam 3 (group 1). Positive zone is anodic and negative zone is cathodic.

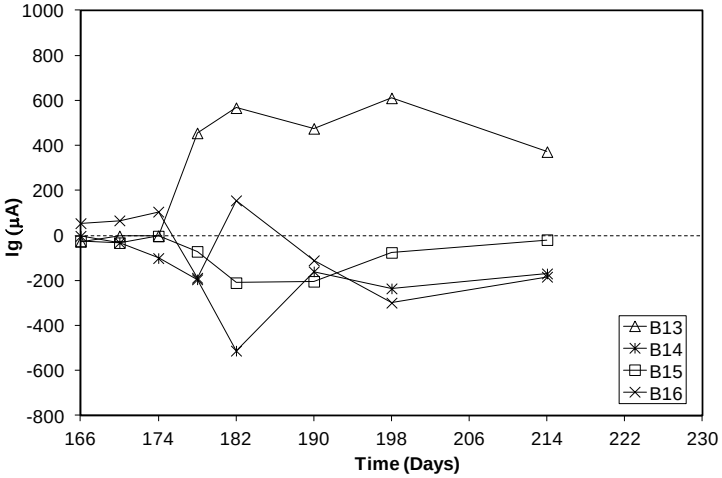

Figure 8. Plot of Ig for bars from Beam 4 (group 1). Positive zone is anodic and negative zone is cathodic.

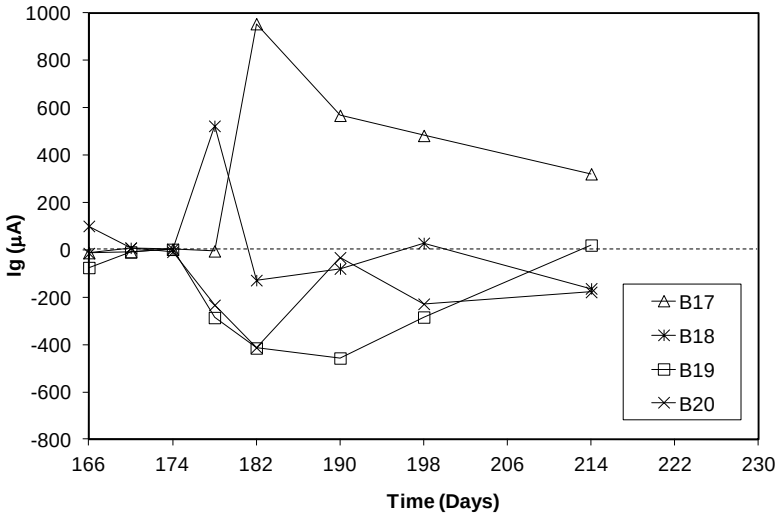

Figure 9. Plot of Ig for bars from Beam 5 (group 1). Positive zone is anodic and negative zone is cathodic.

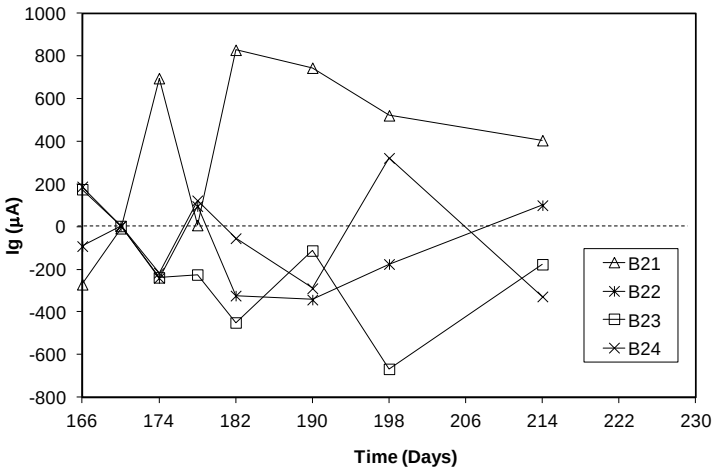

Figure 10. Plot of Ig for bars from Beam 6 (group 1). Positive zone is anodic and negative zone is cathodic.

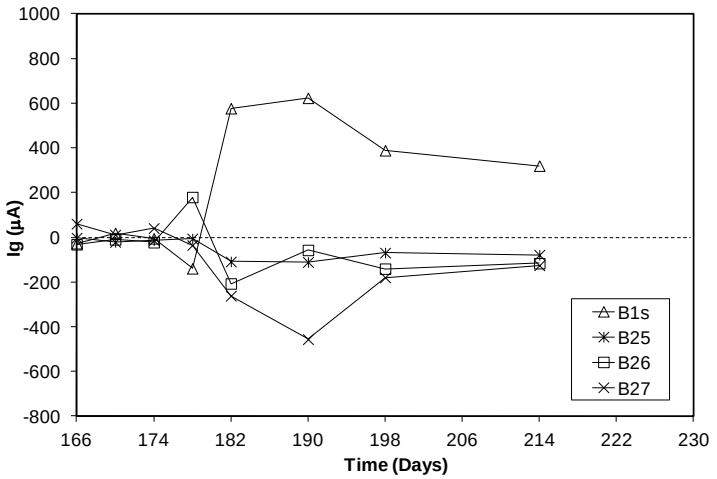

Figure 11. Plot of Ig for from Beam 7 (group 2). Anodic zone is positive and cathodic zone is negative.

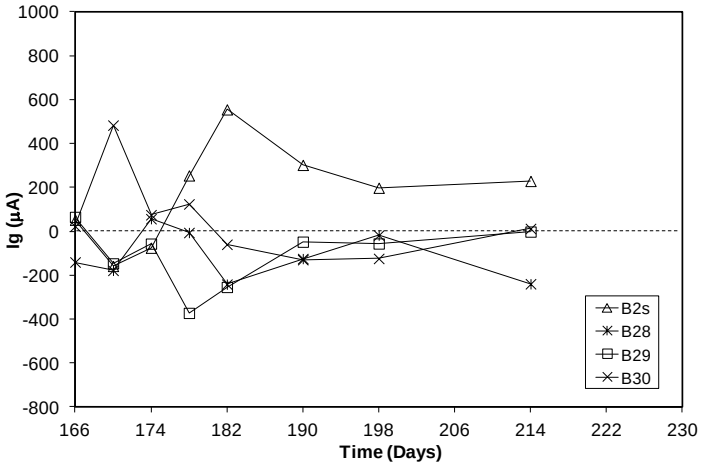

Figure 12. Plot of Ig for from Beam 8 (group 2). Anodic zone is positive and cathodic zone is negative.

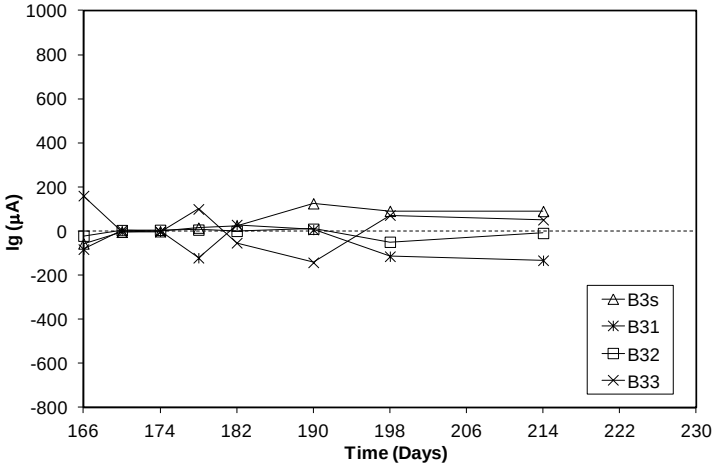

Figure 13. Plot of Ig for from Beam 9 (group 2). Anodic zone is positive and cathodic zone is negative.

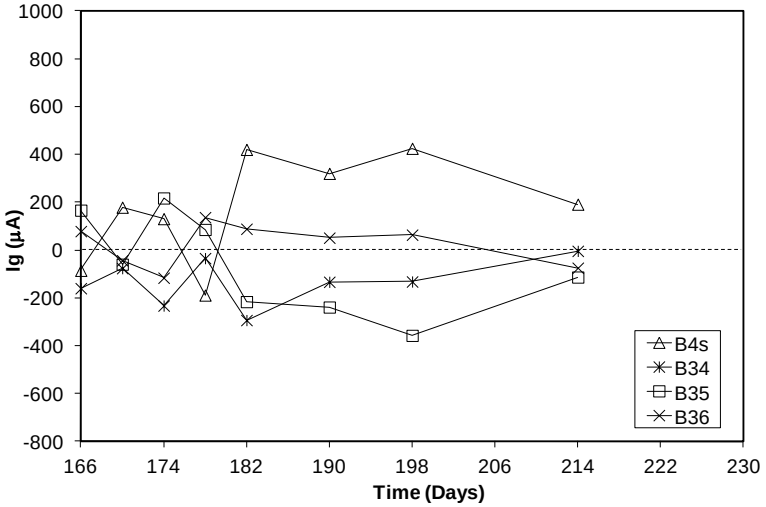

Figure 14. Plot of Ig for from Beam 10 (group 2). Anodic zone is positive and cathodic zone is negative.

On the other hand, figures 11 to 14 show the Ig behavior of beams from Group 2. Similar tendencies to those from Group 1 were observed for bars B1s, B2s, B3s and B4s . Also, most of the rest of the bars in both groups developed and conserved a cathodic behavior.

Until now, plots are showing a galvanic behavior of juxtaposed bars. However, it can also be analyzed the behavior of the coplanar bars as observed in Figures 15 to 18. It is very clear the anodic behavior of the attacked segment compared with the cathodic one of most of the rest of the coplanar segments.

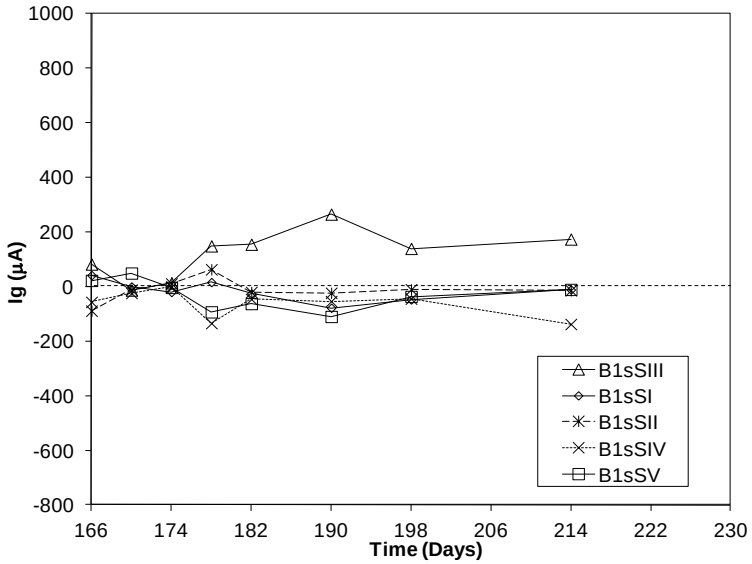

Figure 15. Plot of Ig for the 5 coplanar segments of bar 1s. Anodic zone is positive and cathodic zone is negative.

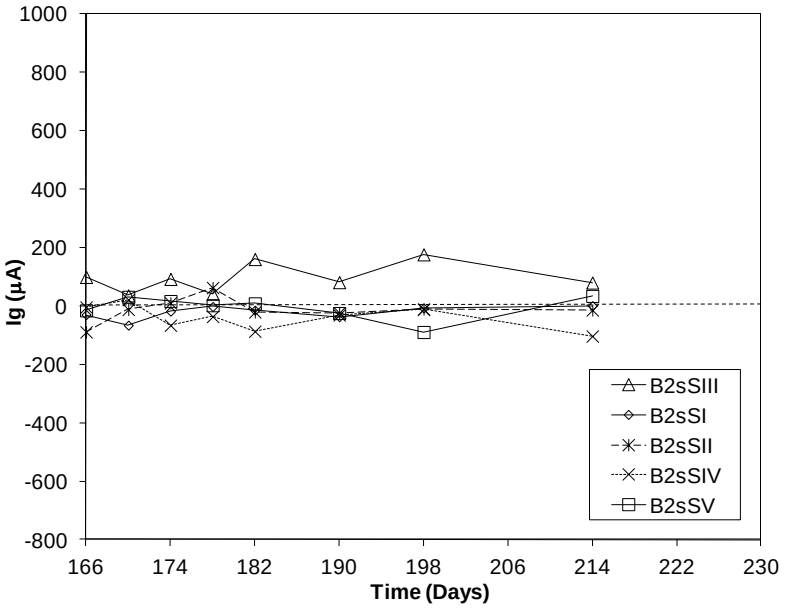

Figure 16. Plot of Ig for the 5 coplanar segments of bar 2s. Anodic zone is positive and cathodic zone is negative.

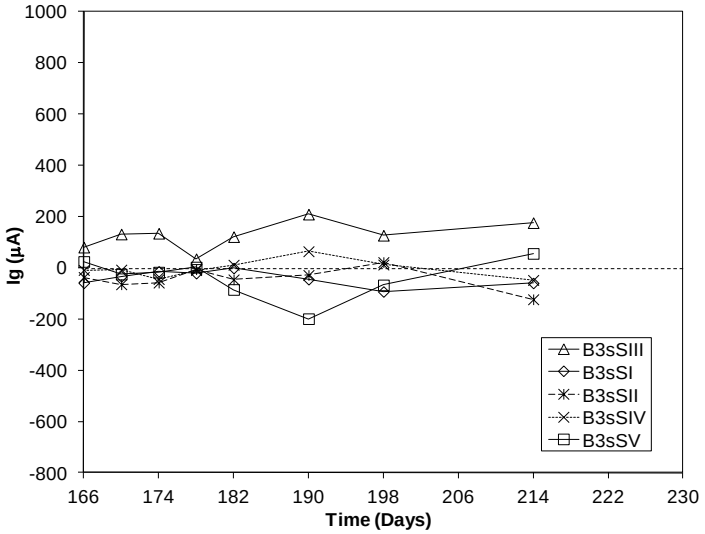

Figure 17. Plot of Ig for the 5 coplanar segments of bar 3s. Anodic zone is positive and cathodic zone is negative.

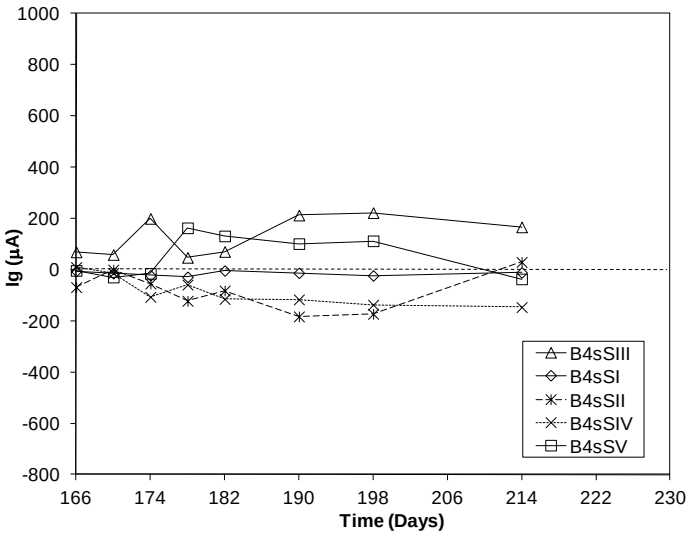

Figure 18. Plot of Ig for the 5 coplanar segments of bar 4s. Anodic zone is positive and cathodic zone is negative.

Once knowing the single galvanic behavior of the beams during the pre-corrosion period, data were prepared and analyzed for the entire described 4 stages. Representative plots of the 4 stages for groups 1 (beam 2) and 2 (beam 7), as well as for segmented bars (B1s from beam 7) can be analyzed in Figures 19, 20 and 21. Then, the measured aA/aC ratio values were calculated and presented in Table 1. These values were calculated by dividing the number of anodes by the number of cathodes for each segmented bar. For example, if we have five segments on the segmented bar and one of them works as an anode, then, the aA/aC ratio is ¼, this is 0.25 and so on. The greatest anodic values found throughout the bar were recorded as Ig.

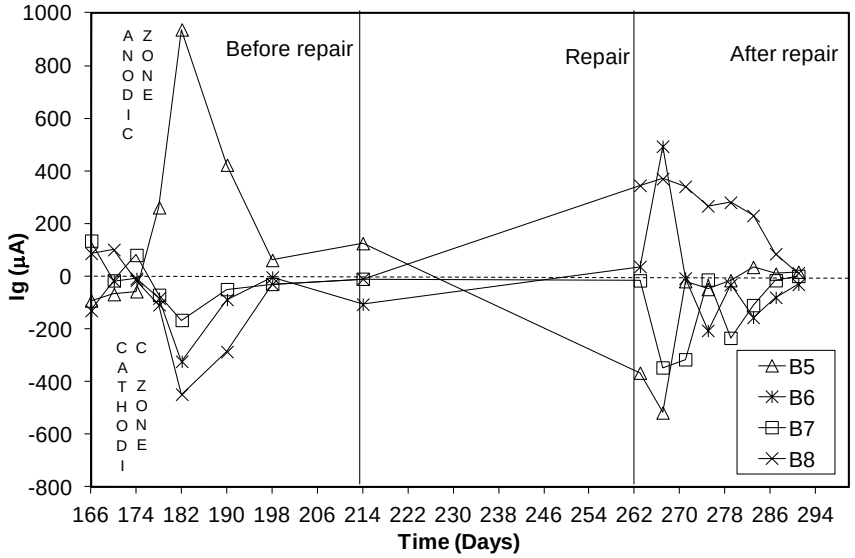

Figure 19. Representative plot of the 4 stages for beam 2, group 1

.

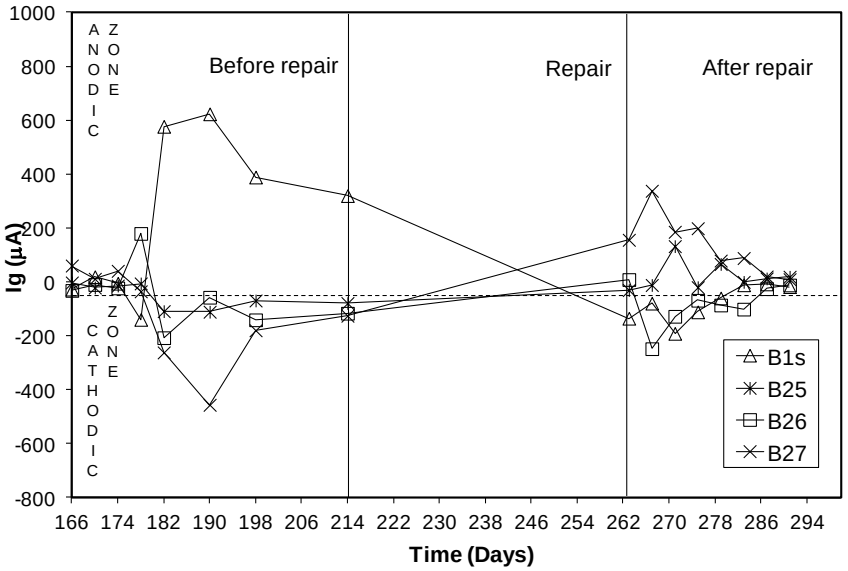

Figure 20. Representative plot of the 4 stages for beam 7, group 2.

The aA/aC ratio varied among the stages in such a way that four relations were observed: 0.25, 0.67, 1.5 and 4. Figure 22 plots the values shown in Table 1, where the galvanic current (Ig) was inversely proportional to the aA/aC area ratio. This behavior is appraised for stages 3 and 4. Such overall tendency was observed based on all of the data recorded for stages 1, 2, 3 and 4, resulting in the following regression equation.

$y= 72.69x^{-0.9835}$, with an R^2 of 0.6065.

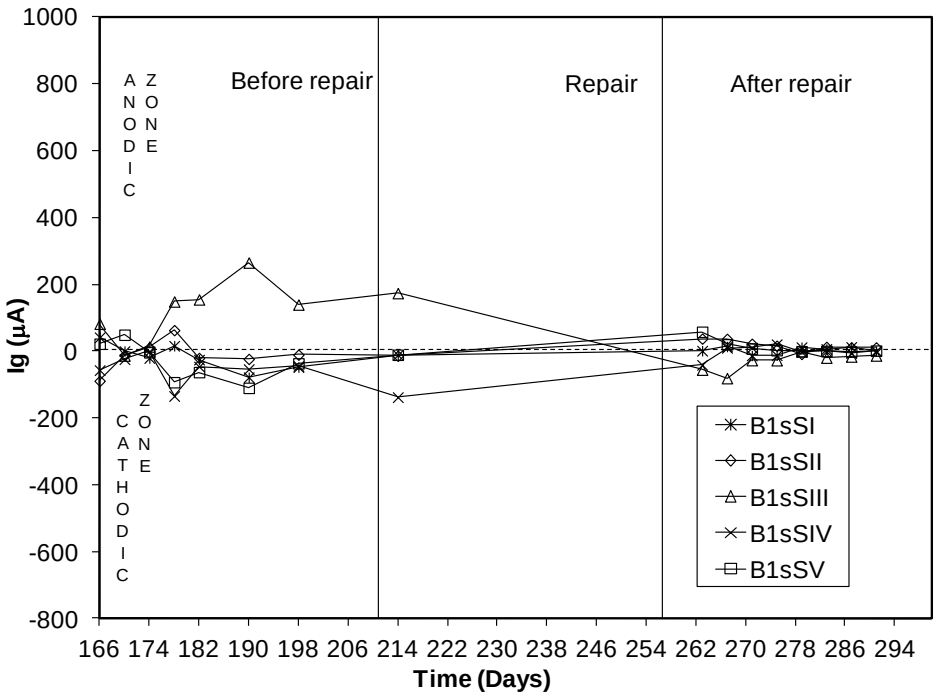

Figure 21. Representative plot of the 4 stages for segmented bar (B1s from beam 7).

Table 1. aA/aC area ratio measurements and corresponding Ig values.

Beam	Stage 1		Stage 2		Stage 3		Stage 4	
	aA/aC	Ig	aA/aC	Ig	aA/aC	Ig	aA/aC	Ig
7	0.25	265.20	0.25	173.70	4.00	36.82	4.00	11.10
8	0.25	176.60	1.50	80.10	4.00	45.65	4.00	2.90
9	0.67	209.00	0.67	175.70	0.67	180.50	0.67	43.40
10	0.67	212.29	0.67	166.09	0.67	173.90	0.67	40.75

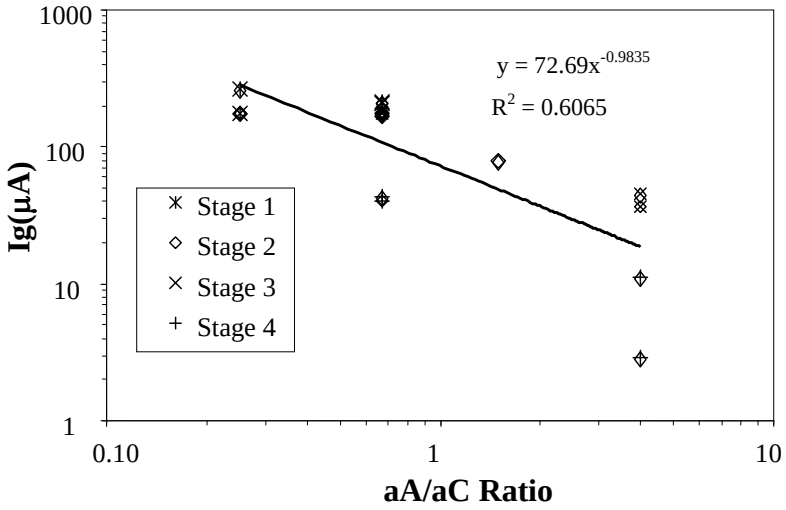

Figure 22. Predicted relationship between a A/aC ratios and Ig values based on a cuadratic regression equation.

The recorded galvanic current values based on the regression equation are shown in Table 2. The aA/aC ratio values ranged from 0.01 to 10, and when ratio values were equal to 5, the difference in the increase of the galvanic current remained almost constant. Differences were not significant when ratio values were greater than 5.

Table 2. Regression equation values when changing the aA/aC area ratios.

Present study	
aA/aC	Ig (μA)
x	$y = 72.69x^{-0.9835}$
0.001	64859.66
0.01	6737.13
0.05	1383.69
0.10	699.80
0.50	143.73
1.00	72.69
5.00	14.93
6.00	12.48
7.00	10.72
8.00	9.40
9.00	8.37
10.00	7.55

4. DISCUSSION

In the present study, galvanic current measurements were carried out and a regression equation was developed based on the recorded data (Figure 22). These data, together with those reported previously by other authors, were used to develop a new regression equation (Figure 23). Five series of data were presented, and two groups identified and classified depending on their behavior. Therefore, two regression equations were obtained: one based on data from Rodriguez [4], Arya [5] and Song [6], and another with data from Andrade [7] and those from this study. Both regressions show a similar tendency, and an almost constant difference among each line of approximately two orders of magnitude was observed. In the case of data reported by Rodriguez, Arya and Song, the regression equation was $y = 0.7537x^{-0.8731}$, with an R^2 of 0.6492. On the other hand, based on data from Andrade [7] and that reported here, the resulting equation was

$y = 85.761x^{-0.7272}$ and the $R^2 = 0.7145$.

The galvanic current values for the two tendency curves are shown in Tables 3 and 4. aA/aC values ranging from 0.001 to 10 were proposed to solve the equation of the curve. It was observed that

when aA/aC = 5, the difference between galvanic current values decreased considerably, and differences were not significant when area ratios were greater than 5.

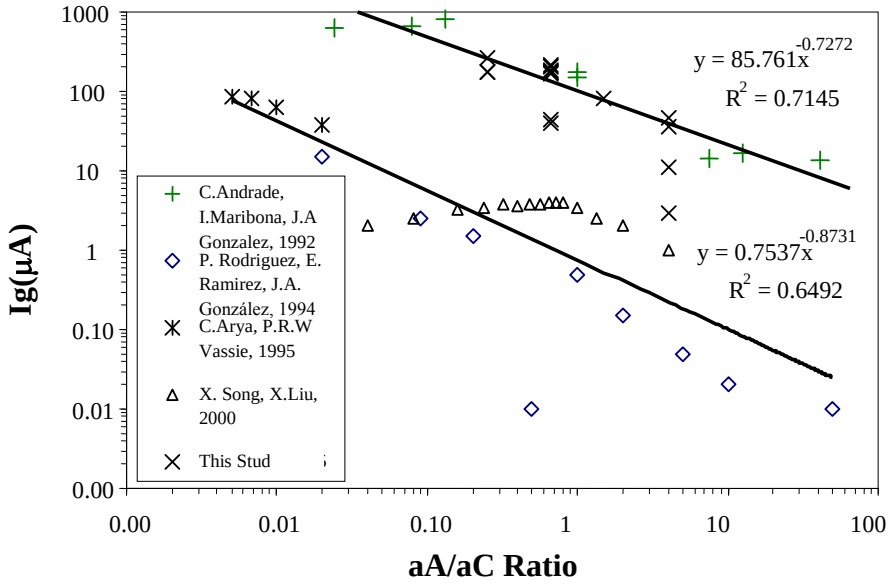

Figure 23. Predicted relationship between aA/aC ratios and Ig values based on a cuadratic regression equation and comparison with data from other authors.

Table 3. Regression equation values when changing the aA/aC ratios reported in the present study.

Present study	
aA/aC	Ig (µA)
X	$y = 85.76x^{-0.7272}$
0.001	13028.36
0.01	2441.69
0.10	457.60
1.00	85.76
5.00	26.61
10.00	16.07

Table 4. Regression equation values when changing aA/aC ratios reported by other authors.

P. Rodriguez, C. Arya, X. Song	
aA/aC	Ig (µA)
X	$y = 0.7537x^{-0.8731}$
0.001	313.69
0.01	42.01
0.10	5.63
1.00	0.75
5.00	0.18
10.00	0.10

5. CONCLUSIONS

The conclusions drawn from this investigation only apply to a set of experimental conditions specific to this study, which suggests that any type of generalization to concrete structures found in natural settings must be made with caution.

a) A strong influence of the anodic/cathodic area ratio on the galvanic behavior of beams before and after local repairs was observed when black steel is replaced by stainless steel. The smaller the aA/aC ratio, the higher the anodic Ig.

b) Before repairing, galvanic couple from tested beams can be very high when chlorides reach the main exposed bar but it decreases when the other bars activate.

c) In practical terms and after repairing, the galvanic current is significant, and therefore detrimental for the beam's structural elements, when the aA/aC ratio is smaller than 5. Under such circumstances, additional measures must be taken in order to control for the galvanic effect when repairing.

ACKNOWLEDGMENTS

The authors thank CINVESTAV of the IPN- Merida and FIUADY for their important and valuable support to this work. M. Córdova thanks CONACYT for financial support to undertake her thesis work which was conducted at CINVESTAV-Merida (M. Sc degree received from FIUADY). The authors are also indebted to M. Balancán who helped with experimental arrangements and measurements. The opinions and findings presented here are of the authors and not necessarily of the supporting organizations.

References

1. R. Baboian, W. France, L. Rowe and J. Rynewicz, *ASTM International*, *ASTM STP* 576 (1976) 20
2. E. Pazini, Evaluation of the Performance of Primers for Reinforcement Protection Against Corrosion Through Electrochemical Technique, Ph. D. thesis, University of Sao Paulo, (1994). (In Portuguesse).
3. P. Castro, E. Pazini, C. Andrade, and C. Alonso, *Corrosion*, 59 (2003) 535.
4. J. Ordaz, Imprimaciones al Acero de Refuerzo como Método de Reparación para Extender la Vida Util Residual de Estructuras de Concreto Armado en Ambiente Marino, Master tesis, Universidad Autónoma de Yucatán, (2001) (In Spanish).
5. P. Rodríguez and E. Ramirez, *Corrosion*, Paper 37 (1994), 66
6. C. Arya and P. Vassie, *Cem. Concr. Res*., 25 (1995) 989
7. X. Song and X. Liu, *ACI Mate. J.*, 97 (2000) 148
8. C. Andrade, I Maribona, et al., *Corr. Sci*., .33 (1992) 237